



## Isotope effect in Ge : a photoluminescence study

P. Etchegoin, J. Weber and M. Cardona

Max-Planck-Institut für Festkörperforschung,  
Heisenbergstrasse 1, D-7000 Stuttgart 80, Germany

W. L. Hansen  
Lawrence Berkeley Laboratory, Berkeley, CA 94720, USA

K. Itoh and E. E. Haller  
UC Berkeley and Lawrence Berkeley Laboratory, Berkeley, CA 94720, USA

(Received July 21, 1992 by T.P. Martin)

Edge photoluminescence data (0.69-0.75 eV) at low temperatures ( $T=1.8$  and  $4.2$  K) were obtained in three isotope enriched Ge crystals ( $\bar{M}=70.1$ ,  $73.95$  and  $75.62$ ) and a natural one ( $\bar{M}=72.59$ ). We observed the energy shifts of the bound exciton, phonon assisted electron-hole liquid and free exciton recombination luminescences as a function of the mean isotope mass. The results are in good agreement with both theoretical estimates using a rigid-ion pseudopotential and some existing experimental information.

### INTRODUCTION

Germanium has a wide natural isotopic spread:  $^{70}\text{Ge}$ ,  $^{72}\text{Ge}$ ,  $^{73}\text{Ge}$ ,  $^{74}\text{Ge}$ , and  $^{76}\text{Ge}$ . In natural Ge (mean atomic weight=72.59) the isotope abundances are (in increasing order of mass): 20.53%, 27.37%, 7.61%, 36.74% and 7.67%. Enriched single crystals with low content of impurities are available nowadays with a very high quality and make Ge almost the ideal candidate to study effects of isotopic disorder on the electron or phonon spectrum [1,2]. In this paper we present photoluminescence data at low temperatures in four samples with different isotopic composition. The replacement of different isotopes in a crystal influences the electron energy states via the electron-phonon (e-p) interaction [3-7]. Likewise, excitons have renormalized energies through the (e-p) interaction that can be observed experimentally [2] as we shall show in the following section. Generally speaking, the isotope and temperature shifts of the electronic gaps have the same origin, i.e. the renormalization of the electronic bands because of the vibrations of the lattice [5,8]. Three main contribution to the electronic band shifts can be distinguished:

i) The expansion of the lattice due to thermal effects or isotope replacement [9] affects the optical gaps. This effect (it exists even at  $T=0$  because of the zero point vibrations) is easily evaluated from the thermal expansion coefficient, bulk modulus and the pressure coefficient of the gap under consideration. The effect on the optical gaps is very small compared to those due to (e-p) interaction which we describe later. It has been estimated in [2] to be of the order of  $\sim 5 \cdot 10^{-5}$  eV at  $T=0$  K. This value is very small when compared with the observed shifts.

ii) The Debye-Waller or electron-two-phonon inter-

action term arises from the simultaneous interaction of two phonons with wave vector  $Q$ , from band  $j$  and polarizations  $\alpha, \beta$ , with an electron in the band  $n$  and wave vector  $k$ . This term is caused by the second-order Hamiltonian for the (e-p) interaction taken to first order. When using the Empirical Pseudopotential Method to calculate the electronic energy bands, this contribution is obtained from a new pseudopotential with Fourier components reduced by Debye-Waller factors ( $\exp[-\frac{1}{6}G^2 \langle u^2 \rangle]$ ), where  $\langle u^2 \rangle$  is the thermal mean phonon amplitude of the atom under consideration. The lowest order expansion of this term ( $\sim 1 - \frac{1}{6}G^2 \langle u^2 \rangle$ ) is in general the only one used in real calculations. The physical meaning of this term is the following: if the lattice were rigid, each atom contributes to the total crystal potential felt by the electrons. The phonons tend to smear the contributions of those atoms with a large average vibration around its equilibrium position.

Note that the Debye-Waller terms tend to suppress the Fourier components of the pseudopotentials with large  $G$ , i.e. the short-range structure of the potential is flattened when the temperature is increased due to the presence of the phonons. The effective potential preserves only the long-range characteristics (small  $G$ ). For this term it suffices to perform a new electronic band structure calculation with the modified pseudopotential using empirical values for the Debye-Waller terms which can be obtained from x-rays diffraction experiments. In this way this procedure can be carried out without any explicit calculation of the phonon branches [10].

iii) The self-energy (SE) contributions to the electron energy renormalization [11] come from the first order (e-p) Hamiltonian to second-order in perturbation theory. Even within the framework of electronic bands

renormalized by Debye-Waller terms, it is still possible for one electron to emit and reabsorb one phonon. The real part of the corresponding self-energy (i.e. the energy shift) is given by [5]:

$$\Delta E_{k,n}^{(SE)} = -\frac{\hbar}{N} \times \sum_{\nu, \nu', n'} \frac{\langle \vec{k}, n | \frac{\partial V}{\partial R_{\alpha, \nu}} | \vec{k} + \vec{Q}, n' \rangle \langle \vec{k} + \vec{Q}, n' | \frac{\partial V}{\partial R_{\alpha, \nu'}} | \vec{k}, n \rangle}{(\epsilon_{\vec{k}, n} - \epsilon_{\vec{k} + \vec{Q}, n'})} \times \left[ e^{-i\vec{Q} \cdot (\vec{r}_\nu - \vec{r}_{\nu'})} (M_\nu M_{\nu'} \Omega_{\vec{Q}}^2)^{-\frac{1}{2}} u_\alpha(\vec{Q} j \nu) u_\beta(\vec{Q} j \nu') \right] \quad (1)$$

with the same notation as in Ref.[5]. The evaluation of these terms requires an explicit calculation of the electronic bands together with a reasonable representation of the lattice dynamics. Explicit calculations have to be performed with a computer code [8]. The Debye-Waller term is usually larger than the self-energy contributions and this explains the reasonable agreement found in earlier calculations [5] using only the term described in (ii).

In the present paper we are interested in the isotope shifts at a fixed temperature. From (ii) and (iii) we find that the isotope effect on the one-electron states (at a given temperature) is proportional to the averaged squared phonon amplitude:

$$|\langle \vec{u}(\vec{Q} j) \rangle|^2 = \frac{\hbar^2}{2M_\nu N \Omega_{\vec{Q} j}} [1 + 2n_{\vec{Q} j}(T)] \quad (2)$$

where  $n_{\vec{Q} j}(T)$  is the Bose-Einstein factor for the phonons (this result holds only if the lowest order expansion of the Debye-Waller term is assumed in (ii)). At room temperature the Bose-Einstein factor can be approximated by  $n_{\vec{Q} j}(T) \sim k_B T / \hbar \Omega_{\vec{Q} j}$  and since  $\hbar \Omega_{\vec{Q} j} \propto M_\nu^{-\frac{1}{2}}$  the averaged phonon amplitude (2) becomes independent of  $M_\nu$ . At low temperatures  $n_{\vec{Q} j}(T) \sim 0$  and then  $|\langle \vec{u}(\vec{Q} j) \rangle|^2 \propto M_\nu^{-1}$ . Hence, isotope shifts in the electronic gaps are observed only at low temperatures and should be related to the average isotopic mass ( $\bar{M}$ ) through:

$$E^{elec} \propto \frac{1}{\sqrt{\bar{M}}} \quad (3)$$

Eventually, absolute values for the isotopic shifts can be compared with theoretical estimates from Ref.[8] using the two terms described in (ii) and (iii) and a rigid-ion pseudopotential. It is interesting to note that phonons behave as if the mass of the lattice were uniform and equal to  $\bar{M}$ . There is no need to consider new features such as the effect of local vibrational modes because partial isotopic substitution is too weak to produce localization of phonons as discussed in Ref.[1]. The relative change in energy as a function of the isotope mass follows directly from (3)

$$\frac{\Delta E^{elec}}{E_{norm}} = -\frac{1}{2} \frac{\Delta \bar{M}}{\bar{M}} \quad (4)$$

where  $E_{norm}$  is the renormalized energy due to the zero point vibrations. So far Eq.(1) holds only for one particle states (electrons or holes) but should remain valid for low binding energy excitons such as those at the indirect edge of Ge. Equation (1) will thus be used for the bound exciton which is observed in photoluminescence at low temperatures [2,12].

The isotope effect on the phonon replicas and the phonon-assisted recombination has two contributions. The energies of the phonons behave like  $\hbar \omega_{ph} \propto 1/\sqrt{\bar{M}}$  and, in addition, the (e-p) interaction contributes with a shift of the electronic gap. It is clear that the interactions explained in (ii) and (iii) can be viewed as the effect of the phonons on the electrons or *vice versa*. Thus, following the same reasoning, the differential shift of a phonon peak is expected to be

$$\Delta(\hbar \omega_{ph}) = \Delta E^{elec} - \frac{\hbar \omega_{ph}}{2} \frac{\Delta \bar{M}}{\bar{M}} \quad (5)$$

Subtracting the experimental phonon energies from the electronic shifts observed in the excitons (electronic part) it is possible to isolate the second term in Eq.(5) and to compare directly with the calculated value taking  $\hbar \omega_{ph}$  from the literature [13]. We shall use Eq.(5) for the phonon replicas of the (e-h) liquid and the phonon-assisted recombination of the free exciton [12].

## EXPERIMENT and DISCUSSION

Edge photoluminescence (PL) data were taken in three enriched samples with average isotopic masses  $\bar{M} = 70.1$ , 73.95 and 75.62 and one sample with the natural isotopic content ( $\bar{M} = 72.59$ ). The enriched samples had gone through a stringent purification process and their impurity content is estimated to be well below  $10^{15} \text{ cm}^{-3}$ . Measurements were performed between 0.69 and

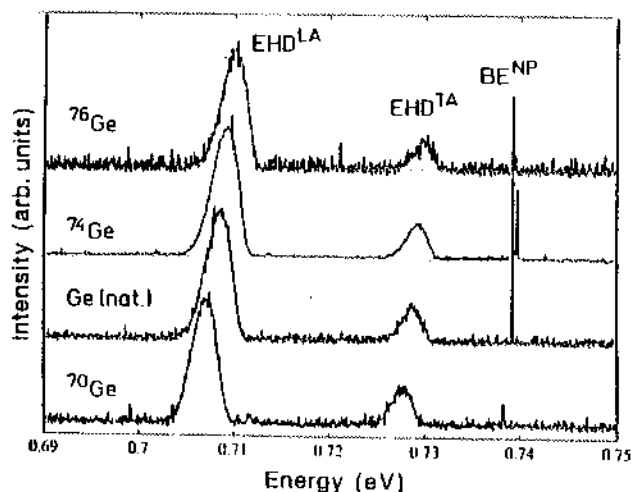


Fig. 1 PL data taken at  $T=1.8 \text{ K}$  in the four different samples ( $\bar{M}=70.1$ , 72.59 (natural), 73.95 and 75.62) of Ge. The three peaks in increasing order of energy correspond to phonon aided recombination of the (e-h) liquid due to LA and TA phonons and exciton bound to neutral impurities respectively. The energy positions of the peaks are given in Table 1.

0.75 eV in a back-scattering configuration. We used a cw Argon laser ( $\lambda = 514.5$  nm) as excitation source with a mean incident power of  $\sim 10$  mW/mm<sup>2</sup>. Measurements were performed in all samples at two temperatures ( $T = 1.8$  and  $4.2$  K) with a resolution varying in the range  $0.1$ – $0.4$  meV. The PL emission was recorded by means of a cooled Ge-detector. In Fig. 1 we show the PL data at  $1.8$  K. At this temperature, three main features can be observed. The sharp lines at  $\sim 0.74$  eV correspond to an exciton bound to a neutral donor. The binding energy of the exciton to the impurity is very small, thus this line can be observed only if  $T \leq 4$  K. The small relative intensity of the bound exciton peaks for  $^{76}\text{Ge}$  and  $^{70}\text{Ge}$  are an indication of the low concentration of neutral impurities and defects in these samples. In Fig. 2 the region near the bound exciton peak is shown in detail. The energy position of the peaks is displayed in Table I. Different noise levels in the data are due to differences in the signal strengths possibly related to differences in the defects and surface conditions. All the samples had been previously polished by mechanical means and etched before the experiment following the prescription of Ref.[14].

The two other peaks in Fig. 1 are the LA and TA phonon replicas of the electron-hole liquid (e-h) recombination. Below a characteristic temperature ( $T \sim 2$  K) excitons undergo a phase transition producing the so called electron-hole drops which also give rise to phonon-assisted radiative recombination. The study of the (e-h) liquid properties has been a subject of active research [15,16] as physical examples of a many-body system of fermions interacting through the Coulomb potential. The weak phonon replicas associated with the (e-h) liquid are only observable at the low temperature and lose their intensity as soon as the temperature reaches  $\sim 3.5 - 4$  K. The line shape of the (e-h) drops luminescence ( $EHD^{LA}$  and  $EHD^{TA}$ ) in Fig. 1 are not symmetric. The line shape for the phonon assisted recombination results from the convolution of the densities of states for holes and electrons modified by the corresponding Fermi distribution at  $T \neq 0$ , i.e.

$$I(h\nu) = I_0 \int_0^\infty |M|^2 g_e(\epsilon) f(\epsilon - E_F^e) \times g_h(h\nu - \epsilon) f(h\nu - \epsilon - E_F^h) d\epsilon \quad (6)$$

where  $|M|^2$  is the matrix element,  $g_{e,h}(\epsilon)$  the densities of states (electrons or holes),  $f(\epsilon)$  the Fermi distribution and  $E_F^{e,h}$  the pseudo-Fermi levels for electrons and holes under the presence of light. The two Fermi levels are not independent since charge neutrality requires  $E_F^e + E_F^h = E_F$  where  $E_F$  is the Fermi level in the dark, at a given temperature. From (6) it can be seen that the luminescence peaks  $EHD^{LA}$  and  $EHD^{TA}$  should rise like  $(h\nu)^2$  at the lower-energy edge. For the purpose of comparing energy shifts as a function of  $\bar{M}$  it suffices to take a fixed point of the line shape for the different isotopes (if the temperature is the same). The values displayed in Table I correspond to the maximum of each peak, respectively. The band edge energy (the energy at which Eq.(6) starts to contribute) is  $\sim 4.8$  meV below that.

In Fig. 3 we show the PL data in the same energy range as in Fig. 1 for  $T = 4.2$  K. In this case the (e-h) liquid emission disappears and the PL signal is dominated by the phonon assisted recombination of the free exciton. The excitons bound to neutral impurities become free at this temperature and, since their  $k$  is not zero, only radiative recombination with emission phonons such that  $\vec{q}_{ph} = \vec{k}$  is allowed ( $\vec{k}_{liquid} \sim 0$ ). These processes can take place as one or multiple-phonon emission. The former governs

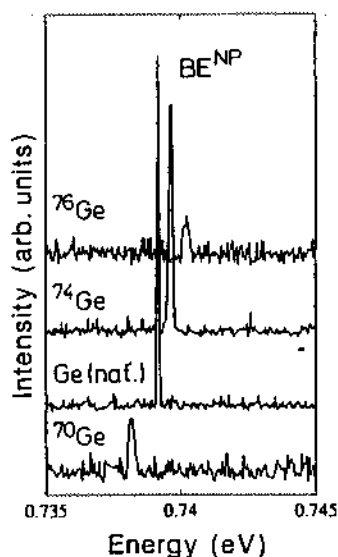


Fig. 2 Bound exciton PL emission from Fig. 1 in an expanded scale. Note the shift of the peaks towards higher energies as a function of  $\bar{M}$ .

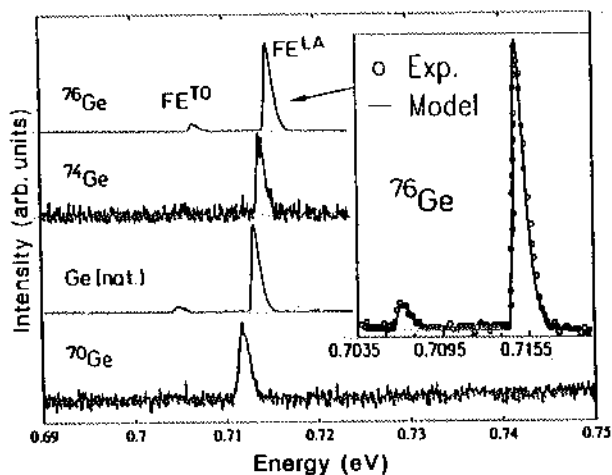


Fig. 3 PL data obtained at  $T = 4.2$  K in the samples of Fig. 1. At this temperature (e-h) liquid emission is lost. The bound exciton can be thermally activated and becomes free. The  $BE^{NP}$  line of Fig. 1 almost disappears although is still distinguishable in  $^{74}\text{Ge}$  and Ge natural. The free exciton can produce now phonon-assisted recombination leading to the phonon replicas shown. All energies are given in Table I. The inset displays the two phonon replicas for  $^{70}\text{Ge}$ . Solid symbols are experimental data while the solid line is a fit to model lineshapes (see text: Eqs.(7), with  $W(\epsilon) = \text{constant}$ , and (9) centered at the appropriate phonon energy).

in general. In Ge the radiative recombination of free excitons in this photon energy region is mediated by LA and TO phonons [2]. The line shape is not symmetric, as expected (a comprehensive review of PL emission and line shapes is given in Ref. [12]). It has been shown [12,17,18] that for one-phonon-assisted emission of the free exciton the spectral distribution of the PL line is given by

$$F(h\omega) \sim \epsilon^{\frac{1}{2}} \exp(-\epsilon/K_B T) W(\epsilon), \quad (7)$$

where  $W(\epsilon)$  is the transition probability rate and

$$\epsilon = h\omega - E_{ex} + h\omega_{ph}, \quad (8)$$

with  $E_{ex}$  the energy of the exciton equal to binding energy plus kinetic energy. The transition probability rate is proportional to the square of the (e-p) coupling constant. The phonon recombination through LA phonons is allowed whilst that through TO phonons is forbidden. The reason for this is that the recombination involves transitions from the  $\Gamma_2'$  to  $L_1$  minima. Decomposing  $\Gamma_2'$  into irreducible representations of  $C_{3v}$  one obtains  $L_2'$ . Since  $L_1 \otimes L_2' = L_2'$ , only transitions involving LA phonons ( $L_2'$  symmetry) are allowed. In this case (LA phonons) the (e-p) matrix element can be taken as a constant. Therefore, the spectral emission is given by (7) with  $W(\epsilon) = \text{constant}$ . For the TO-aided recombination shown in Fig. 3 the analysis is as follows: At  $T=4.2$  K the kinetic energy of the excitons is small and the (e-p) coupling constant can be assumed to be linear in  $\bar{q}_{ph}$ , i.e.  $W(\epsilon) \propto |\bar{q}_{ph}|^2 \propto \epsilon$  and the spectral distribution  $F(h\omega)$  becomes

$$F(h\omega) \sim \epsilon^{\frac{3}{2}} \exp(-\epsilon/K_B T). \quad (9)$$

The inset in Fig. 3 shows a blowup of the phonon replicas in  $^{76}\text{Ge}$  with some experimental points and a fit with the spectral distributions (7) (with  $W(\epsilon) = \text{constant}$ ) and (9) centered around  $h\omega_{LA}$  and  $h\omega_{TO}$  (Eq.(8)), respectively. The relative intensities are fitted so as to exhibit the relative amplitudes found experimentally. The asymmetry of the line shapes is well reproduced. The maximum of  $F(h\omega)$ , at a given temperature, occurs when  $\epsilon = 1/2 K_B T$  for the LA phonon and  $\epsilon = 3/2 K_B T$  for the TO. Hence, from (8) we found  $E_{ex} \sim 7.11$  meV for natural Ge at  $T=4.2$  K. The absolute energies of the maximum of the observed phonon replicas in Fig. 3 are given in Table I for the four samples. The position of the peaks can be usually determined within ~5% of the resolution but is limited in some cases by noise. Note that the fit shown in the inset of Fig. 3 for  $FE^{TO}$  and  $FE^{LA}$  implies only one free parameter, namely the relative intensity of the peaks. Knowing  $h\omega_{TO}$  and  $h\omega_{LA}$  from the literature [13] and using the energy position of the maximum for  $FE^{TO}$  and  $FE^{LA}$  and the known temperature ( $T=4.2$  K), the exciton energy  $E_{ex}$  in (8) is fixed. Therefore, only the relative intensity remains as a free parameter for the fit. However, the curve in the inset of Fig. 3 was obtained assuming  $T=5.1$  K in order to reproduce the experimental broadening (the increase with respect to the nominal  $T=4.2$  K is probably due to laser heating; it could also be fictitiously induced by the splitting of the indirect exciton [19]). In Fig. 4 we summarize the isotope shifts for all the observed PL peaks at  $T=1.8$  and  $4.2$  K. From the best linear fit of the bound exciton luminescence at  $T=1.8$  K we can ob-

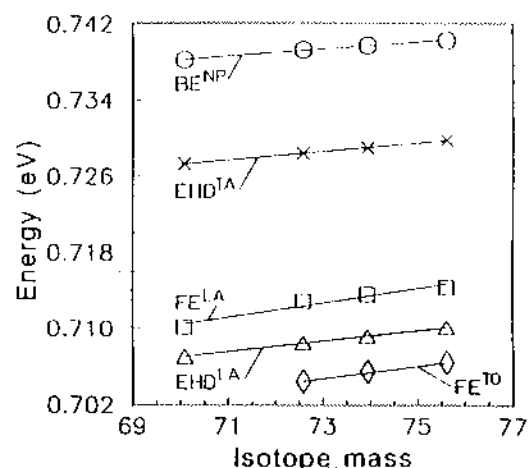


Fig. 4 Energy position of the PL peaks shown in Figs. 2 to 4 at  $T=1.8$  and  $4.2$  K. The lines represent best linear fits in each case (see text).

tain  $\Delta E^{BE}$  as shown in Fig. 4 and Table I. Inserting this value in Eq.(4) and  $\Delta \bar{M}=5.52$  we can calculate the renormalization energy  $E_{norm}$  (4) of the electrons [8]. We compare in Table I this value with existing theoretical calculations [8] including both, Debye-Waller and self-energy terms, using a rigid-ion pseudopotential. The values are given in Table I: good agreement is found. Also the results compare well with the extrapolation to  $T=0$  of  $E_{gap}(T)$  measured at higher temperatures, as expected [6,20]. Once the shift due to the electronic part is known, we can use Eq.(5) to evaluate the expected shift in the phonon-aided peaks. Since the second term in (5) is proportional to the phonon energy, independent values obtained with inelastic neutron scattering [13] were used to find  $\Delta(h\omega_{phonon})$ . The values are displayed in Table I and the comparison with the measured ones is again satisfactory.

As mentioned before, phonon frequencies follow the trivial mass dependence  $\propto (\bar{M})^{-\frac{1}{2}}$ . However, departures from this law are observed experimentally and depend on the phonon under consideration. This effect is produced by isotopic disorder and has been studied with Raman spectroscopy [1] and infrared transmission spectroscopy [22]. The energy of the phonons should contain an isotope-disorder induced self-energy. Calculations of this effect with the coherent potential approximation (CPA) have been performed [21,22]. They predict a negligible contribution for LA and a disorder-induced phonon self-energy of  $\sim -0.2$  meV for TO phonons ( $TO_K-TO_L$ ) (Fig. 4 in Ref.[1]) in natural Ge when compared with a hypothetical pure isotopic sample of the same mass. We have attempted to find evidence for this shift in the following manner: The phonon-assisted recombinations of the free exciton in Fig. 3 have not only the mass dependence of the phonons included but also the electronic shift (Eq.(5)). We removed the electronic part by subtracting the energies of  $FE^{TO}$  and  $FE^{LA}$  from that of the bound exciton (Fig. 3). The values so obtained differ slightly from the absolute phonon energies. The data can be slightly shifted so that the energies for TO and LA coincide with the values reported in the literature [13]. In this way we obtain the data plotted in Fig. 5. The two solid lines are functions of the form  $C/(\bar{M})^{\frac{1}{2}}$  ( $C$  is an adjustable param-

TABLE 1. Absolute energies and relative shifts for the photoluminescence lines of the bound exciton ( $BE^{NP}$ ), phonon replicas of the electron-hole liquid ( $EHD^{TA}$  and  $EHD^{LA}$ ), and phonon assisted recombination of the free exciton ( $FE^{LA}$  and  $FE^{TO}$ ). The experimental conditions are given in the footnotes (all energies are in meV).

Isotope	$BE^{NP}$	$EHD^{TA}$	$EHD^{LA}$	$FE^{LA}$	$FE^{TO}$
$^{70.1}\text{Ge}$	$738.28 \pm 0.03^a$	$727.3 \pm 1.3^a$	$707.1 \pm 1.2^a$	$710.2 \pm 0.2^b$	—
$^{72.59}\text{Ge (nat.)}$	$739.20 \pm 0.03^a$	$728.4 \pm 1.2^a$	$708.5 \pm 1.2^a$	$713.0 \pm 0.1^b$	$705.0 \pm 0.3^b$
$^{73.95}\text{Ge}$	$739.66 \pm 0.03^a$	$728.9 \pm 1.1^a$	$709.2 \pm 1.1^a$	$713.7 \pm 0.3^b$	$705.7 \pm 0.5^b$
$^{75.62}\text{Ge}$	$740.23 \pm 0.03^a$	$729.8 \pm 1.4^a$	$710.2 \pm 1.4^a$	$714.5 \pm 0.1^b$	$706.8 \pm 0.3^b$
Energy shift	$\Delta E^{BE}$	$\Delta(\hbar\omega_{TA})^{EHD}$	$\Delta(\hbar\omega_{LA})^{EHD}$	$\Delta(\hbar\omega_{LA})^{FE}$	$\Delta(\hbar\omega_{TO})^{FE}$
Experimental	$2.05 \pm 0.00^{a,c}$	$2.47^{a,d}$	$3.12^{a,e}$	$3.22^{b,f}$	$1.93^{b,g}$
Calculated	$2.26^{h,i}$	$2.43^j$	$3.17^k$	$3.17^k$	$1.86^l$
Energy renormalization <sup>m</sup>	Experimental		Theory		
	$-51.9(2.1)^{a,d,n}$		$-60.65^i$		

<sup>a</sup>  $T=1.8$  K.

<sup>b</sup>  $T=4.2$  K.

<sup>c</sup> Obtained using  $\Delta E$  from the best linear fit of the  $BE^{NP}$  peak in Fig. 4.

<sup>d</sup> Obtained using the best linear fit of the  $EHD^{TA}$  peak in Fig. 4.

<sup>e</sup> Same as (d) with the best linear fit for  $EHD^{LA}$ .

<sup>f</sup> Same as (d) with the best linear fit for  $FE^{LA}$ .

<sup>g</sup> Same as (d) with the best linear fit for  $FE^{TO}$ .

<sup>h</sup> Theoretical value from Ref.[8].

<sup>i</sup> Pseudopotential-bond-charge-model.

<sup>j</sup> Calculated using Eq.(6) with  $\Delta E = \Delta E^{BE}$  (exp.) and  $\hbar\omega_{TA} = 7.8$  meV from Ref.[13].

<sup>k</sup> Same as (j) with  $\hbar\omega_{LA} = 27.75$  meV from Ref.[13].

<sup>l</sup> Same as (j) with  $\hbar\omega_{TO} = 36.0$  meV from Ref.[13].

<sup>m</sup> Energy renormalization of the  $\Gamma-X$  indirect electronic gap due to electron-phonon interaction at  $T=0$

<sup>n</sup> For  $\bar{M} = 70.1$ .

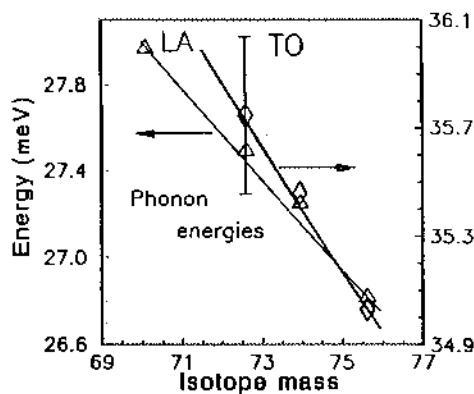


Fig. 5 LA and TO phonon energies. The experimental points were obtained from the data of Fig. 3 ( $FE^{TO}$  and  $FE^{LA}$ ). The values so obtained were shifted so that the energies of TO and LA in the natural sample coincide with those reported in the literature [13]. The solid lines were obtained using  $\hbar\omega_{\text{phonon}} = C/\sqrt{\bar{M}}$ , ( $C$  = adjustable parameter). The departure from this law is a signature of isotopic disorder; no evidence of isotopic disorder is observed (see text).

ter). We choose  $C$  in each case so that the curve coincides with the experimental data for  $^{70}\text{Ge}$  in the case of LA and with the experimental point for  $^{70}\text{Ge}$  for TO. No evidence of isotope disorder induced self-energies is found. We note, however, that error bars for the TO phonon frequencies are  $\sim \pm 0.3$  meV and the expected self-energy,  $-0.2$  meV, falls well within these error bars. We are at present growing a crystal with 50%  $^{70}\text{Ge}$  and 50%  $^{76}\text{Ge}$  which should lead to a four times larger self-energy, discernable within the error margin of the present work.

In addition to these experiments we also performed ellipsometric measurements of the  $E_1 - E_1 + \Delta_1$  gaps at low temperatures ( $T \sim 10$  K) and PL of the direct gap. Our ellipsometry data for the isotope shifts of the  $E_1 - E_1 + \Delta_1$  gaps did not improve the results already reported in Ref.[8], except for the addition of a new sample ( $^{74}\text{Ge}$ ). Although more satisfactory (due to the better quality of the  $^{70}\text{Ge}$  sample), the total shifts of both gaps (obtained with an appropriate model for the critical points) are  $\sim 5.5 \pm 3$  meV going from  $\bar{M} = 70.1$  to  $\bar{M} = 75.62$ . This is similar to the values reported in Ref.[8] but about three times larger than the theoretical ones.

In conclusion, we observed the isotope effect on the PL spectra of four different Ge samples and found good agreement with both, theoretical calculations [8], and some previous experimental data [2,13]. In the only previous report of this effect (Ref.[2]), using luminescence

science, the LA and TO phonon replicas of the (e-h) liquid in one enriched sample ( $\bar{M} = 75.69$ ) were compared with the natural one. In Ref.[23] similar results were reported for the lowest (indirect) gap of diamond.

#### Acknowledgments

Thanks are due to H. Hirt, M. Siemers and P. Wurster for technical help and to H. D. Fuchs for a critical reading of the manuscript.

#### REFERENCES

- [1] H. D. Fuchs, C. H. Grein and M. Cardona, *Solid State Commun.* **82**, 225 (1992).
- [2] V. F. Agekyan, V. M. Asnin, A. M. Kryukov, I. I. Markov, N. A. Rud', V. I. Stepanov and A. B. Churilov, *Sov. Phys. Solid State* **31** (12), 2082 (1989).
- [3] V. S. Kogan, *Sov. Phys. Usp.* **5**, 951 (1963).
- [4] V. G. Plekhanov, V. A. Pustovarov, A. O'Connell-Bronin, T. A. Betenokova and S. O. Cholak, *Sov. Phys. Solid State* **18**, 1422 (1976).
- [5] M. Cardona and S. Gopalan in *Progress on Electron Properties of Solids*, ed. by R. Girlanda (Kluwer, Dordrecht, The Netherlands, 1989), p.51, and references therein.
- [6] P. Lautenschlager, P. B. Allen and M. Cardona, *Phys. Rev. B* **31**, 2163 (1985); S. Gopalan, P. Lautenschlager and M. Cardona, *ibid.* **35**, 5577 (1987).
- [7] M. L. Cohen and D. J. Chadi in *Handbook of Semiconductors*, ed. by M. Balkanski (North-Holland, Amsterdam, 1980), Vol. 2, p. 155.
- [8] S. Zollner, M. Cardona and S. Gopalan, *Phys. Rev. B* **45**, 3376 (1991).
- [9] R. C. Buschert, A. E. Merlini, S. Pace, S. Rodriguez and M. Grimsditch, *Phys. Rev. B* **38**, 5219 (1988).
- [10] J. S. Reid, *Acta Cryst.* **A39**, 1 (1983).
- [11] H. Y. Fan, *Phys. Rev.* **82**, 900 (1951).
- [12] H. B. Bech and E. W. Williams in *Semiconductors and Semimetals*, ed. by R. K. Willardson and A. C. Beer (Academic Press, New York, 1972), Vol. 8, p. 181.
- [13] M. S. Skolnick and W. Kress in *Landolt-Börnstein*, ed. by K. H. Hellwege (Springer, Berlin, 1982), III/17a p.101.
- [14] D. E. Aspnes and A. A. Studna, *Phys. Rev. B* **47**, 985 (1983).
- [15] J. C. Hensel, T. G. Phillips, G. A. Thomas, and T. M. Rice in *Solid State Physics*, ed. by H. Ehrenreich, F. Seitz and D. Turnbull (Academic, New York, 1977), Vol. 32.
- [16] *Electron-Hole Droplets in Semiconductors in Modern Problems in Condensed Matter Series*, ed. by C. D. Jeffries and L. V. Keldysh, (North Holland, Amsterdam, 1983), Vol. 6.
- [17] G. D. Mahan and B. Segall in *II-VI Semiconducting Compounds* (Proc. Int. Conf.), (Benjamin, Amsterdam, 1967), p. 349.
- [18] B. Segal and G. D. Mahan, *Phys. Rev.* **171**, 935 (1967).
- [19] A. Frova, G. A. Thomas, R. E. Miller and E. O. Kane, *Phys. Rev. Lett.* **34**, 1572 (1975).
- [20] P. Lautenschlager, P. B. Allen and M. Cardona, *Phys. Rev. B* **33**, 5501 (1986).
- [21] A. A. Berezin and A. M. Ibrahim, *Chem. Phys.* **19**, 407 (1988).
- [22] H. D. Fuchs, C. H. Grein, C. Thomsen, M. Cardona, W. L. Hansen, E. E. Haller and K. Itoh, *Phys. Rev. B* **43**, 4835 (1991) and H. D. Fuchs, C. Grein, M. Bauer and M. Cardona, *Phys. Rev. B* **45**, 4065 (1992).
- [23] A. T. Collins, S. C. Lawson, G. Davies and H. Kanda, *Phys. Rev. Lett.* **65**, 891 (1990).